

The nucleon-nucleon potential in the chromodielectric soliton model: Statics

W. Koepf and L. Wilets

Department of Physics, FM-15, University of Washington, Seattle, Washington 98195

S. Pepin and Fl. Stancu

Université de Liège, Institut de Physique B.5, Sart Tilman, B-4000 Liège 1, Belgium

(Received 3 February 1994)

We study the nucleon-nucleon interaction in the framework of the chromodielectric soliton model (CDM). Here, the long-range parts of the non-Abelian gluon self-interactions are assumed to give rise to a color-dielectric function which is parametrized in terms of an effective scalar background field. The six-quark system is confined in a deformed mean field through an effective nonlinear interaction between the quarks and the scalar field. The CDM is covariant, respects chiral invariance, leads to absolute color confinement, and is free of the spurious long-range van der Waals forces which trouble nonrelativistic investigations employing a confining potential. Six-quark molecular-type configurations are generated as a function of deformation and their energies are evaluated in a coupled channel analysis. By using molecular states instead of cluster model wave functions, all important six-quark configurations are properly taken into account. The corresponding Hamiltonian includes the effective interaction between the quarks and the scalar background field and quark-quark interactions generated through one gluon exchange treated in Coulomb gauge. When evaluating the gluonic propagators, the inhomogeneity and deformation of the dielectric medium are taken into account. Results for the adiabatic nucleon-nucleon potential are presented, and the various contributions are discussed. Finally, an outlook is given on how, in the next stage of our investigation, dynamical effects will be incorporated by employing the generator coordinate method.

PACS number(s): 24.85.+p, 21.30.+y, 13.75.Cs, 12.39.Ba

I. INTRODUCTION

The nucleon-nucleon interaction is one of the most basic problems of nuclear physics. There exists extensive experimental information, from N - N scattering data and the properties of the deuteron, but no single theoretical picture seems to be able to describe the relevant physics for all internuclear distances. In N - N phenomenology, both relativistic and nonrelativistic, one treats the nucleons as elementary particles interacting through a two-body potential which is either local or includes some nonlocality through momentum and state dependence in the interaction. The general features of that potential, i.e., the short-distance core and the long-range attraction, have been known for over forty years.

Already in 1935, Yukawa [1] suggested that the attraction was due to the exchange of an intermediate mass, strongly interacting particle, the subsequently discovered pion. This led to the development of meson field-theoretic models which today form the most accurate phenomenological description of the N - N interaction (see Ref. [2] for an excellent overview). In these models, one treats the nucleons as elementary particles with an empirical form factor, and their interactions are mediated through one boson exchange (OBE) plus two pion exchange (TPE), where the latter is frequently simulated by a (fictitious) scalar meson.

Within these descriptions, the long-range ($r \gtrsim 1.5$ fm) part of the N - N interaction is controlled by one pion exchange, while the intermediate range ($0.5 \text{ fm} \lesssim r \lesssim$

1.5 fm) attraction is dominated by OBE and TPE. The short-range ($r \lesssim 0.5$ fm) repulsion is the "mystery" region in such prescriptions. It has been described by hard or soft cores, or form factors, both of the order of 0.5 to 0.8 fm, or by the exchange of vector mesons which, however, have a range of $1/m_\omega \approx 0.2$ fm.

The advent of QCD and quark models has lifted the veil of mystery from the short range N - N interaction exposing a new level of simplicity. However, the system is no longer just a two-body, but at least a six-body, entity and more properly a field-theoretical problem. The quark core of nucleons is of the order of 0.7 fm (a rms radius of 0.5 fm), and one thus expects the quark substructure to be effective within a range of N - N separations of up to about 1 fm.

A description of the N - N interaction within the framework of quark degrees of freedom has been the subject of much research. The ideal venture would be a lattice gauge theory calculation (see, e.g., [3]), but we are quite far from that stage, and therefore we have to rely on modeling. We mention, nonexhaustively, several different avenues which have been explored in that context: nonrelativistic constituent quark models [4], relativistic current quark models, such as the MIT bag [5] and various soliton models [6], string models, and the topological Skyrme model [7-9]. There are many varieties under each category, and we will not attempt to review them all here, but rather recommend the reader to see the review articles by Oka and Yazaki [10], Myhrer and Wroldsen [11], or Shimizu [12].

In addition to the various methods which have been employed to model nucleon-nucleon interactions, one has to further distinguish between static and dynamical calculations. In the static calculations, a local N - N potential is obtained in Born-Oppenheimer [13] (adiabatic) approximation from the energy difference of a deformed six-quark bag and two separated noninteracting nucleons. Nonadiabatic calculations, on the other hand, yield a nonlocal interaction through a consideration of the dynamics involved. In the latter category, usually the resonating group [14] or the generator coordinate method [15] is applied.

Quark models hold promise for giving a good description for short and intermediate range, but beyond, say, 1 fm the interaction, although in principle describable in terms of quarks, is much more easily represented by mesonic models, with the nucleonic substructure giving rise to form factors for the meson-nucleon couplings.

The ultimate object of our study is not only to reproduce the two-body data such as N - N phase shifts and bound state properties of the deuteron, but also to quantify the quark substructure of nuclei. With respect to the latter, we will describe the collision process as an act of fusion followed by a separation into three-quark clusters, and this will be used in conjunction with the independent pair model of nuclei to obtain, e.g., quark structure functions. With this in mind, the main aspects of our current project can be described as follows:

(i) We employ the chromodielectric soliton model [16,17], which respects covariance, yields absolute color confinement and is free of the color van der Waals problem [18] (which is inherent to most nonrelativistic calculations). In addition, one gluon exchange is evaluated with a “confined” gluonic propagator.

(ii) The six-quark wave function is expanded in terms of “molecular” states [19], including all configurations based on the two lowest spatial single-particle states. This allows for consideration of basis states normally omitted in the cluster model and which have been demonstrated to be important in decreasing the energy of a spherical six-quark system in variational calculations [20,21].

(iii) Dynamics will be handled through the generator coordinate method [22], which leads to a set of coupled integral equations. It has been claimed [6] that a significant part of the short-range repulsion is due to dynamics, and the absence of a repulsive core in some early calculations is now seen as an artifact of the adiabatic approximation [23,24]. In addition, the effective interaction is nonlocal in terms of the N - N separation parameter.

(iv) In order to reproduce two-body properties, beyond a certain internuclear distance we will attach the interaction we derive to a phenomenological local OBE potential (cf. for example Ref. [25]). We could, however, also consider extending our calculation more deeply into the intermediate-range region by either including quantum surface fluctuations and introducing configurations of the form $q^7\bar{q}$ in addition to our q^6 basis states, or by explicitly allowing mesonic degrees of freedom.

In this first of a planned series of papers, we are mostly concerned with the introduction of the model and a pre-

sentation of the formalism we use. Therefore, we restrict ourselves to an adiabatic, or static, approximation. We calculate $\langle\alpha|H|\alpha\rangle$, where α is the separation or deformation parameter, including diagonalization with respect to the various six-quark configurations. We defer steps (iii) and (iv) to subsequent papers in this series [26,27].

The outline of this work is as follows. In Sec. II, we review some of the earlier work on the chromodielectric soliton model and construct three-quark nucleons. In Sec. III, we describe how we generate single-quark wave functions through a constrained mean field calculation. Section IV is devoted to the “molecular” states which form the basis for the six-quark configurations we consider. Section V describes the treatment of the one gluon exchange, and in Sec. VI we present the results of our numerical calculations. Finally, we summarize, conclude, and give an outlook on our future work in Sec. VII.

II. THE MODEL

The chromodielectric model [16,17] is an evolution of the Friedberg-Lee nontopological soliton model [28]. Its Lagrangian is the same as the fundamental QCD Lagrangian, supplemented by a scalar field which is supposed to simulate the gluonic condensate and other scalar structures which inhabit the complicated physical vacuum. It is assumed that the scalar field, which has a nonvanishing vacuum expectation value, parametrizes the bulk of nonperturbative effects which arise due to the nonlinearity of QCD.

The extra degrees of freedom introduced by the scalar field are redundant, and in order to avoid double counting we do not include diagrams which correspond to structures with the quantum numbers of the σ field. Since the model parameters are readjusted at each level of approximation to fit key physical data, one might hope that as the level of sophistication of the calculations is increased, one would find a decoupling of the σ degrees of freedom and would thus be left with pure QCD. But, we are currently far from that stage, and although the model has its basis in QCD, we regard it as phenomenological.

The model Lagrangian

$$\mathcal{L} = \mathcal{L}_q + \mathcal{L}_\sigma + \mathcal{L}_G, \quad (1)$$

with

$$\mathcal{L}_q = \bar{\psi} (i\gamma^\mu D_\mu - m_q) \psi, \quad (2a)$$

$$\mathcal{L}_\sigma = \frac{1}{2} \partial_\mu \sigma \partial^\mu \sigma - U(\sigma), \quad (2b)$$

$$\mathcal{L}_G = -\frac{1}{4} \kappa(\sigma) F_{\mu\nu}^c F^{\mu\nu c}, \quad (2c)$$

is covariant and, for massless quarks, satisfies chiral symmetry. It differs in that respect from most effective quark models, such as the MIT [29], Friedberg-Lee [28], or Nielsen-Patkos [30] models, which explicitly violate chiral symmetry through the interaction of the quarks with some scalar field.

Here, m_q is the current quark mass matrix; for the rest of this investigation, we set $m_q \equiv 0$. In addition, $F_{\mu\nu}^c$ is the color-SU(3) gauge field tensor, and $U(\sigma)$ is the self-

interaction energy of the scalar field which is taken to be of the form

$$U(\sigma) = \frac{a}{2!}\sigma^2 + \frac{b}{3!}\sigma^3 + \frac{c}{4!}\sigma^4 + B. \quad (3)$$

The quartic form of $U(\sigma)$ would assure renormalizability if κ were a constant [31]. The bag pressure B (which corresponds to the “bag constant” of the MIT model) is chosen such that $U(\sigma)$ has a minimum and vanishes at the scalar field’s vacuum expectation value, i.e., $U(\sigma_v) = U'(\sigma_v) = 0$. One defines

$$U''(\sigma_v) \equiv m_{\text{GB}}^2, \quad (4)$$

where m_{GB} is identified with the mass of the lowest 0^{++} glueball state. The scalar field furthermore governs the chromodielectric properties of the medium through $\kappa(\sigma)$, and in order to guarantee absolute color confinement and a regular behavior as $\sigma \rightarrow \sigma_v$, the dielectric function must satisfy

$$\begin{aligned} \kappa(\sigma_v) &= \kappa'(\sigma_v) = \kappa'(0) = 0 \\ \text{and} \\ \kappa(0) &= 1. \end{aligned} \quad (5)$$

We choose the form (with $x = \sigma/\sigma_v$)

$$\kappa(\sigma) = 1 + \theta(x)x^n[nx - (n+1)], \quad (6)$$

and set $n = 2$ for our present investigation.

Although the quarks are massless and there is no direct quark-sigma coupling, they still acquire a self-energy, and

hence an effective mass, through their interactions with the gluon field. This confinement mechanism has been studied for a uniform dielectric function [17] as well as a cavity model in which κ is unity at the center and goes to zero outside the bag [32]. It was shown [17] that the quarks’ self-energy acquires an asymptotic form which increases as κ decreases and becomes infinite as $\kappa \rightarrow 0$. This corresponds to a realization of *spatial confinement*, since this mass is “color blind.”

Color confinement, on the other hand, arises through the enclosure of the quark cavity by the physical vacuum where the dielectric function goes to zero [31]. Note that $\kappa \rightarrow 0$ also ensures that there are no spurious color van der Waals forces. Furthermore, the gluonic propagator depends on σ through $\kappa(\sigma)$ and is thus also “confined.”

Inspired by the results of these studies [16,17,32], we introduce an *effective coupling* between the quarks and the scalar field,

$$\mathcal{L}_{q\sigma} = -g_{\text{eff}}(\sigma) \bar{\psi} \psi, \quad (7)$$

with

$$g_{\text{eff}}(\sigma) = g_0 \sigma_v \left(\frac{1}{\kappa(\sigma)} - 1 \right), \quad (8)$$

which is designed to simulate spatial confinement already at the mean field level.

The effective energy functional is given by

$$H = \int d^3\mathbf{r} \mathcal{H}(\mathbf{r}), \quad (9)$$

where

$$\mathcal{H} = \psi^\dagger \left[\boldsymbol{\alpha} \cdot (\mathbf{p} - \frac{1}{2}g_s \boldsymbol{\lambda}^c \cdot \mathbf{A}^c) + \beta g_{\text{eff}}(\sigma) + \frac{1}{2}g_s \boldsymbol{\lambda}^c \cdot A_0^c \right] \psi + \frac{1}{2} \left(\frac{\partial \sigma}{\partial t} \right)^2 + \frac{1}{2} |\nabla \sigma|^2 + U(\sigma). \quad (10)$$

This must be supplemented by the field equations for A_0^c and \mathbf{A}^c , which will be given in Sec. V.

In order to fit the parameters of the model, we construct a self-consistent solution for the nucleon. We treat the scalar field classically and drop the gluonic terms when determining the quark wave function or the scalar field. See Ref. [33] for more details. We incorporate certain approximate recoil corrections [34], which should be compared with methods using projection and boost [35]. Of the five parameters involved [a , b , and c in $U(\sigma)$, g_0 in g_{eff} , and the strong coupling constant α_s], three are fixed by fitting the nucleon mass, the Δ mass, and the proton rms charge radius. This leaves two free parameters, for which we choose the dimensionless quantities $f \equiv b^2/ac$ and c .

For $f = 3$, the bag pressure B vanishes, which generates “hard” bags with a thin surface. For $f = \infty$, the quadratic term in $U(\sigma)$ disappears, and $\sigma = 0$ turns from a second minimum to an inflection point. This yields “soft” bags with a thick surface. In general, for increas-

ing c , the glueball mass and the bag pressure increase, the agreement in the axial vector coupling g_A , which is inherently too small by about 10 percent, improves, but the proton’s magnetic moment μ_p (which is also consistently underestimated) grows to differ more from its experimental value. Table I gives an overview of the corresponding quantities for the various parameter sets under consideration.

As already remarked, we work in the one gluon exchange approximation. Since for both the nucleon and the Δ all of the quarks are in the same spatial state, and the entire system is a color singlet, the total (mutual plus self) color-electrostatic energy is zero. The color-magnetic interaction, on the other hand, is responsible for the N - Δ mass splitting. In general, part of this energy difference should be attributed to the different pion dressing of the nucleon and the Δ , but since presently our soliton does not contain any pionic effects, we disregard this contribution. As usual [36], the magnetic self-energy contribution is neglected and no intermediate excitations

TABLE I. Results of a self-consistent mean field calculation for the nucleon for various parameter sets as characterized by $f \equiv b^2/ac$ and c , adjusted to yield the same recoil corrected proton rms charge radius of 0.83 fm and recoil corrected nucleon mass of 939 MeV. The quantities listed are the 0^{++} glueball mass m_{GB} , the bag pressure B , the nucleon's axial vector coupling constant g_A , and the proton's magnetic moment μ_p . The strong coupling constant α_s is adjusted to yield the mass of the Δ resonance of 1232 MeV, employing either a free or a confined gluonic propagator.

f	c	m_{GB} (MeV)	B (MeV/fm ³)	g_A	μ_p (μ_N)	α_s	
						Free	Confined
3.0	30000	2933	0	1.24	2.21	3.36	1.32
	10000	1948	0	1.21	2.29	3.36	1.42
	3000	1254	0	1.18	2.34	3.34	1.57
	1000	734	0	1.12	2.42	2.90	2.25
3.2	30000	2501	40	1.21	2.28	3.49	1.43
	10000	1787	32	1.20	2.31	3.48	1.46
	3000	1214	22	1.19	2.34	3.45	1.56
	1000	783	12	1.15	2.38	3.18	2.03
∞	30000	2355	67	1.21	2.31	3.66	1.47
	10000	1755	62	1.21	2.31	3.64	1.50
	3000	1243	52	1.20	2.32	3.58	1.59
	1000	874	38	1.18	2.35	3.49	1.79

of the quarks into higher spatial orbitals are taken into account. The evaluation of the N - Δ mass splitting allows the adjustment of the strong coupling constant, and the corresponding results are given in Table I. Hereby, a ‘‘confined’’ gluonic propagator is used, i.e., the explicit dependence of the gluonic field equations on the dielectric function $\kappa(\sigma)$ is taken into account. For details see Sec. V and Ref. [36]. For comparison, we also show the values of α_s which we obtain by using a free propagator, i.e., by setting $\kappa \equiv 1$.

III. CONSTRAINED MEAN FIELD APPROXIMATION

The starting point of any evaluation of a multidimensional potential energy surface and the input to any calculation employing the generator coordinate method is a wave function which is characterized by a set of deformation parameters, which in the following will be denoted collectively as α . In our case, the α describe the static configuration of a system of six quarks and the corresponding deformed scalar σ field, which is treated quantum mechanically through the coherent state approximation. Consideration of various six-quark configurations (see Sec. IV for more details) allows for each deformation the construction of a complete basis, which is indicated by a set of state vectors $|\alpha, n\rangle$.

In general, these state vectors are generated by means of a constrained mean field calculation, i.e., by extremizing the expectation value of the total Hamiltonian, as given by $\langle \alpha | H | \alpha \rangle$, with respect to a variational wave function for the quarks and a coherent state for the scalar field, subject to the constraints

$$\langle \alpha | Q | \alpha \rangle = Q_0, \quad (11)$$

where the Q are some moments of the quark distribution as defined through

$$Q = \int d^3\mathbf{r} \bar{\psi}(\mathbf{r}) \mathbf{q}(\mathbf{r}) \psi(\mathbf{r}), \quad (12)$$

for some chosen set $\mathbf{q}(\mathbf{r})$. In the above, we have dropped the label ‘‘ n ’’ for simplicity, and in the following, we limit ourselves to a one-dimensional deformation parameter space and consider zero-impact trajectories (or central collisions) only. The constrained mean field equations then assume the form

$$\{\alpha \cdot \mathbf{p} + \beta [g_{\text{eff}}(\sigma(\mathbf{r})) - \lambda q(\mathbf{r})] - \epsilon_n\} \psi_n = 0, \quad (13)$$

$$-\nabla^2 \sigma + \frac{dU(\sigma)}{d\sigma} + \frac{dg_{\text{eff}}(\sigma)}{d\sigma} \langle \bar{\psi} \psi \rangle = 0, \quad (14)$$

where $\langle \bar{\psi} \psi \rangle$ is the six-quark scalar density and λ is a Lagrange multiplier imposing the subsidiary condition of Eq. (11). All gluonic terms have been dropped from the above equations, and the label n identifies the different single-particle quark states.

Instead of specifying the constraint function $q(\mathbf{r})$ explicitly and solving the above pair of equations simultaneously and self-consistently, we specify the function

$$[g_{\text{eff}}(\sigma(\mathbf{r})) - \lambda q(\mathbf{r})] \equiv \mathcal{V}_\alpha(\mathbf{r}) \equiv g_{\text{eff}}(\sigma_\alpha(\mathbf{r})) \quad (15)$$

for each value of the collective deformation parameters α . $\mathcal{V}_\alpha(\mathbf{r})$ then plays the role of an external potential generating the wave function for the quarks, and it is expressed in terms of a scalar field with a prescribed deformation, $\sigma_\alpha(\mathbf{r})$.

Following Schuh *et al.* [6], we construct the field $\sigma_\alpha(\mathbf{r})$ by folding a Yukawa-shaped smoothing function with the union (for $\alpha > 0$) or intersection (for $\alpha < 0$) of two spheres whose centers are separated by the distance $|\alpha|$, i.e.,

$$\sigma_\alpha(\mathbf{r}) = \sigma_v - \sigma_0 \int T_\alpha(\mathbf{r}') f(|\mathbf{r} - \mathbf{r}'|) d^3\mathbf{r}', \quad (16)$$

$$T_\alpha(\mathbf{r}) = \begin{cases} \theta[R(\alpha) - |\mathbf{r} - \hat{\mathbf{z}}\alpha/2|] & \text{for } z \geq 0, \\ \theta[R(\alpha) - |\mathbf{r} + \hat{\mathbf{z}}\alpha/2|] & \text{for } z < 0, \end{cases} \quad (17)$$

$$f(r) = \frac{\Gamma^2 e^{-\Gamma r}}{4\pi r}, \quad (18)$$

where σ_v is the vacuum expectation value of the scalar field, and where $\alpha > 0$ corresponds to prolate deformations and $\alpha < 0$ to oblate deformations. In this, we restrict ourselves to a physically reasonable three-parameter representation of the external potential $\mathcal{V}_\alpha(\mathbf{r})$. The underlying parameter space is, of course, infinite dimensional.

The parameters R , Γ , and σ_0 are determined from our self-consistent solution for the nucleon, such that the corresponding scalar field of two free nucleons is well approximated at asymptotic deformations, i.e.,

$$\sigma_{\alpha \rightarrow \infty}(\mathbf{r}) \rightarrow \sigma_N(\mathbf{r} - \hat{\mathbf{z}}\alpha/2) + \sigma_N(\mathbf{r} + \hat{\mathbf{z}}\alpha/2) - \sigma_v. \quad (19)$$

In order to select a definite path in configuration space, the field strength σ_0 and the surface parameter Γ are kept constant and the radius $R = R(\alpha)$ is varied in such a way that the volume of the six-quark cavity is independent of its deformation and remains fixed at the value of two nucleonic volumes. In Fig. 1, we show the field $\sigma_\alpha(\mathbf{r})$ obtained in that manner for four different α 's.

Selecting this particular path in the geometrical configuration space spanned by R , Γ , and σ_0 is equivalent to treating the scalar field as an incompressible liquid. In order to check this approximation, we constructed self-consistent stationary eigenstates of the total Hamiltonian for a spherically symmetric bag, i.e., for $\alpha = 0$. Our findings, which will be discussed in Sec. VI, show that the quality of the ‘‘constant volume’’ approximation is quite remarkable.

The potential $\mathcal{V}_\alpha(\mathbf{r})$ serves to generate a set of single-particle quark states, which are determined from the eigenvalue equation (13). Here, we limit ourselves to the

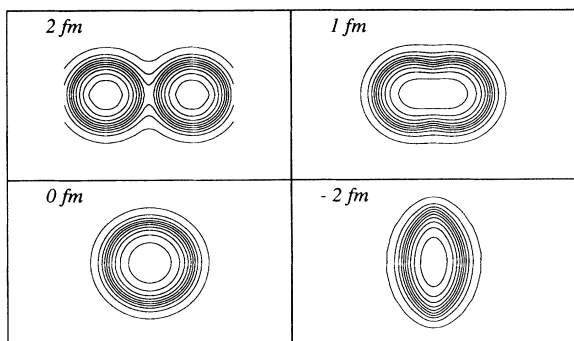


FIG. 1. The scalar field, $\sigma_\alpha(\mathbf{r})$ of Eq. (16), from which the single-quark wave functions are generated, for four different values of the deformation parameter α between 2 fm and -2 fm. The fields correspond to the parameter set with $f = 3$ and $c = 10\,000$, and are shown with equal increments between adjacent contours.

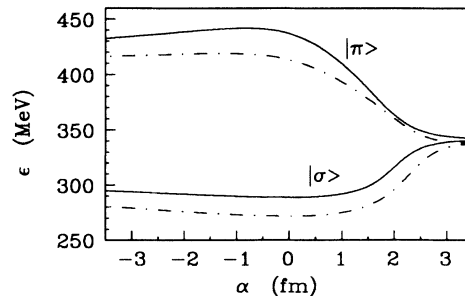


FIG. 2. The eigenenergies of the lowest single-particle states of positive and negative parity determined from Eq. (13) for values of the magnetic quantum number of $m = \pm 1/2$. Results are shown for two particular parameter sets with $c = 10\,000$ and $f = 3$ (solid line) or $f = \infty$ (dot-dash line).

lowest states of positive and negative parity, denoted by $|\sigma\rangle$ and $|\pi\rangle$, and to values for the single-particle magnetic quantum number of $m = \pm 1/2$. The corresponding eigenenergies, ϵ_σ and ϵ_π , are shown in Fig. 2 for two particular parameter sets ($c = 10\,000$; $f = 3$ and $f = \infty$). Figure 2 depicts the increasing binding of the positive parity state for small α , as well as the convergence of both levels for separating bags, i.e., as $\alpha \rightarrow \infty$. Then, the two states become degenerate and turn into linear combinations of $|R\rangle$ and $|L\rangle$, corresponding to an s state in either bag. As $\alpha \rightarrow 0$, the single-particle states evolve to $\sigma \rightarrow s_{1/2}$ and $\pi \rightarrow p_{3/2}$, respectively.

IV. QUARK MOLECULAR BASIS STATES

The classification and construction of antisymmetric six-quark basis states is a central part of any study of the N - N system in terms of quark degrees of freedom. Incorporating all possible degrees of freedom [color (C), orbital motion (O), spin (S), and isospin (T)] we use a classification scheme based on $SU(4)$ spin-isospin symmetry, as introduced by Harvey [37], to construct configurations which are totally antisymmetric with respect to the interchange of any pair of particles, i.e., have Young symmetry [1⁶]. Using fractional parentage coefficients [38] we can reduce the six-body matrix elements of the effective Hamiltonian to linear combinations of one- and two-body matrix elements.

The novelty with respect to Harvey’s scheme and other similar studies lies in the choice of the orbital share of the wave function. In most previous calculations, the cluster model has been used (see Ref. [11] for a review), which describes the orbital degrees of freedom in terms of two separate three-quark clusters centered at the locations of the two respective nucleons, denoted in the following as $|R\rangle$ and $|L\rangle$. In this investigation, on the other hand, we use ‘‘molecular orbitals’’ [19], where the spatial single-particle states are wave functions of a static single-particle Hamiltonian, such as obtained from constrained Hartree-Fock or soliton mean field theories, and which in our case are the two lowest orbitals of either parity,

$|\sigma\rangle$ and $|\pi\rangle$. It is obvious that the molecular states are orthogonal at any separation, whereas the cluster model states are not. The latter even overlap completely for vanishing internucleon separation, $\langle R|L\rangle|_{\alpha=0} = 1$. Note also that in the cluster model, the limit $\alpha \rightarrow 0$ requires special care in the normalization of the various symmetry configurations [19]. Otherwise some contributions are mistakenly left out, as was the case in Refs. [5], [23], and [37], for example.

In Refs. [20] and [21], results for a united six-quark bag obtained with cluster model wave functions were compared with corresponding calculations employing molecular basis states and, in particular, the constituent quark model and the MIT bag model were investigated. In both cases, the authors found that the ground state energies were substantially lowered through the use of molecular orbitals. The reason for this is that configurations of the type $|R^n L^{6-n}(n \neq 3)\rangle$, which are absent in a cluster model basis, proved to be quite important.

The only sectors which are compatible with $L = 0$ N - N partial waves are $T = 0$, $S = 1$ and $T = 1$, $S = 0$ (Ref. [39]). The relevant orbital symmetries are then $[f]_O = [6]$ and $[42]$ assuming that each nucleon is asymptotically in a $[f]_O = [3]$ state. For the spin-isospin channels, on the other hand, only the $[f']_{TS} = [51]$ and $[33]$ evolve into asymptotic dibaryon states for large internucleon separations. As all other $[f']_{TS}$ states couple very weakly to the latter [20,21], they can safely be disregarded for the N - N problem. This leaves the following states (employing the notation of Ref. [19]):

$$\begin{aligned} |1\rangle &= |NN\rangle, \\ |2\rangle &= |\Delta\Delta\rangle, \\ |3\rangle &= |CC\rangle, \\ |4\rangle &= |42^+[6]_O [33]_{TS}\rangle, \\ |5\rangle &= |42^+[42]_O [33]_{TS}\rangle, \\ |6\rangle &= |42^+[42]_O [51]_{TS}\rangle, \\ |7\rangle &= |51^+[6]_O [33]_{TS}\rangle, \end{aligned} \quad (20)$$

for the basis of our truncated Hilbert space. The first three form the ‘‘physical’’ basis in Harvey’s investigation of the N - N interaction [37], and they contain solely configurations which are asymptotically of the type $|R^3 L^3\rangle$. The other four are asymptotically of the form $|R^4 L^2 + R^2 L^4\rangle$ or $|R^5 L + RL^5\rangle$, denoted as 42^+ and 51^+ , respectively. Configurations of that type do not occur in the standard cluster model.

V. ONE-GLUON EXCHANGE

We treat quark-gluonic interactions in the one-gluon exchange approximation. At this level, we are not confronted with the problem of double counting, since colorless structures which are already represented by the scalar field begin with two-gluon exchange or the excitation of $q\bar{q}$ pairs.

In addition, the non-Abelian terms in the QCD gauge field tensor $F_{\mu\nu}^c$ have been neglected, since higher order effects (which arise due to the non-Abelian character of

QCD) are assumed to be simulated by the scalar field. The field equations therefore linearize and become identical to Maxwell’s equations in an inhomogeneous medium [31]. In this approximation, we find from Eqs. (2a) and (2c)

$$\partial^\mu (\kappa(\sigma) (\partial_\mu A_\nu^c - \partial_\nu A_\mu^c)) = J_\nu^c, \quad (21)$$

where the total quark color-current operator is

$$J_\nu^c = \frac{g_s}{2} \bar{\psi} \gamma_\nu \lambda^c \psi, \quad (22)$$

with $g_s = \sqrt{4\pi\alpha_s}$, and Gell Mann’s color-SU(3) matrices are denoted by λ^c . The gluonic fields are explicitly affected by the scalar field through $\kappa(\sigma)$. As the dielectric is constructed in such a way as to ensure absolute color confinement, the resulting gluonic propagators will also be ‘‘confined,’’ and there will be no gluons propagating outside the solitonic bags.

In order to solve the field equations, we choose the Coulomb, or transverse, gauge,

$$\nabla \cdot (\kappa \mathbf{A}) = 0, \quad (23)$$

which decouples A_0 in (21) through

$$-\nabla \cdot \kappa \nabla A_0 = J_0. \quad (24)$$

The field equation for the spatial components of A_μ^c reads

$$\kappa \partial_t^2 \mathbf{A} - \nabla^2 \kappa \mathbf{A} + \nabla \times (\mathbf{A} \times \nabla \kappa) = \mathbf{J}_t, \quad (25)$$

where the transverse current is defined by means of

$$\mathbf{J}_t = \mathbf{J} - \kappa \nabla \partial_t A_0. \quad (26)$$

We note that due to the scalar nature of the medium, the field equations are diagonal in the color indices, which have hence been omitted in Eqs. (23)–(26). From these equations, we can furthermore deduce the mutual and self-interaction energies between the quarks which arise due to the OGE, and finally evaluate their contributions to the one-body and two-body parts of the effective Hamiltonian. Respective diagrams are shown in Figs. 3(a) and 3(b), and the corresponding matrix elements

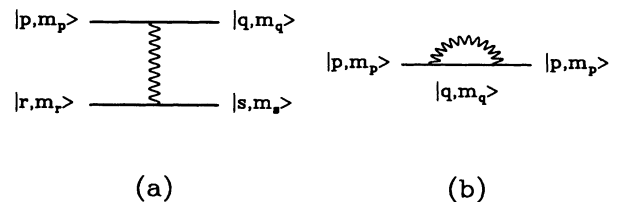


FIG. 3. Typical one-gluon exchange diagrams that contribute to the gluonic share of the effective Hamiltonian. The diagram shown in (a) corresponds to the two-body mutual interactions, while the graph depicted in (b) corresponds to one-body self-interactions.

are evaluated by first determining the gluon propagator “in medium.” We follow here Bickeboeller *et al.* [40], as subsequently corrected by Tang and Wilets [41] where, however, the corrections in Ref. [41] do not affect the matrix elements used here.

The part of the OGE interactions that arises from the time component of the gluonic field is responsible for the realization of color confinement, and the part of the OGE interactions that stems from the spatial components of the gluonic field generates the color-magnetic hyperfine interaction which, in turn, produces the N - Δ mass splitting. As usual, the self-interaction terms have been included in the time part of the OGE and have been neglected for the spatial contributions. This is in accordance with the minimal self-energy prescription of the MIT bag model [42]. Only when taking the color-electrostatic self-energy diagrams arising from the time component of the gluonic field into account, the color-electrostatic interaction between two well separated nucleonic color singlets vanishes, as is required by color neutrality [5].

In addition, the OGE matrix elements from the color-

magnetic hyperfine interaction are significantly smaller than the ones generated by the color-electrostatic interaction. The reason for this reduction is that the latter always involve the “small” lower components of the relativistic quark spinors. Inasmuch as the magnetic interaction is not directly involved in color confinement, we simplify our calculations by using a free (i.e., $\kappa \equiv 1$) tensor propagator and an effective $\alpha_s \rightarrow \alpha_s^{\text{free}}$ adjusted to yield the experimental N - Δ splitting.

VI. RESULTS AND DISCUSSION

In the following, we will present our results for the adiabatic, local N - N potential, $V_{ad}^{NN}(\alpha) = \langle \alpha | H | \alpha \rangle - 2E_N$, obtained in Born-Oppenheimer approximation from the energy difference of a deformed six-quark bag and two well separated noninteracting nucleons. The underlying effective Hamiltonian can be separated into two distinct contributions, $\langle H_1^{\text{bag}} \rangle$ and $\langle H_{\text{OGE}} \rangle$. The nongluonic one-body term has the form

$$\begin{aligned} \langle H_1^{\text{bag}} \rangle = & \epsilon_\sigma \langle b_\sigma^+ b_\sigma \rangle + \epsilon_\pi \langle b_\pi^+ b_\pi \rangle - \frac{1}{2} \int d^3\mathbf{r} \left(\frac{dg_{\text{eff}}(\sigma)}{d\sigma} \sigma \langle \bar{\psi} \psi \rangle + \frac{dU(\sigma)}{d\sigma} \sigma - 2U(\sigma) \right) \\ & + \int d^3\mathbf{r} [g_{\text{eff}}(\sigma) - g_{\text{eff}}(\sigma_\alpha)] \langle \bar{\psi} \psi \rangle, \end{aligned} \quad (27)$$

with the scalar quark density

$$\langle \bar{\psi} \psi \rangle \equiv \langle b_\sigma^+ b_\sigma \rangle \bar{\psi}_{\sigma m} \psi_{\sigma m} + \langle b_\pi^+ b_\pi \rangle \bar{\psi}_{\pi m} \psi_{\pi m}. \quad (28)$$

$\langle H_1^{\text{bag}} \rangle$ arises from the single-particle energies [ϵ_σ and ϵ_π of Eq. (13) and depicted in Fig. 2] and the scalar field σ from Eq. (14) as well as the external potential generating the quark wave functions $g_{\text{eff}}(\sigma_\alpha)$ of Eq. (15). Note the distinction between the scalar field σ , which is an explicit dynamical degree of freedom, and the auxiliary quantity σ_α , which, as outlined in Sec. III, is only used to generate single-quark wave functions with a certain deformation.

In addition, there is the one gluon exchange contribution,

$$\langle H_{\text{OGE}} \rangle = \langle H_1^\sigma \rangle + \langle H_1^\pi \rangle + \langle H_2^{\sigma\sigma\sigma\sigma} \rangle + \langle H_2^{\pi\pi\pi\pi} \rangle + \langle H_2^{\sigma\sigma\pi\pi} \rangle + \langle H_2^{\sigma\pi\pi\sigma} \rangle + \langle H_2^{\pi\sigma\sigma\pi} \rangle, \quad (29)$$

with the one-body self-energy terms, $\langle H_1^\sigma \rangle$ and $\langle H_1^\pi \rangle$, and the various two-body contributions $\langle H_2^{pqrs} \rangle$ allowed by parity conservation. The corresponding diagrams are shown in Fig. 4. It is important to note that in the OGE self-energy terms only the color-electrostatic interaction was taken into account, and that the $\sigma - \pi - \sigma$ and $\pi - \sigma - \pi$ “off-diagonal” terms are essential in providing for the confinement of the color-electric flux [5].

The adiabatic potential will be shown as a function of the deformation parameter α , which was introduced in Sec. III [see Eqs. (16)–(18)]. For large prolate deformations, α coincides with the true nucleon-nucleon separation. For smaller deformations, however, only a dynamical calculation employing, e.g., the generator coordinate method, can yield the transformation between α and the exact internucleon separation. In Fig. 5 we show the dependence of the internucleon separation r on the de-

formation parameter α , as taken from Ref. [6]. There, the N - N interaction was investigated in terms of quark degrees of freedom within the Friedberg-Lee soliton model, but no gluonic effects were included. We note that the spherical configuration, $\alpha = 0$, corresponds to a still finite internucleon separation, and that $r \rightarrow 0$ is approached for oblate deformations, i.e., for $\alpha < 0$. Although the exact form of the transformation $r(\alpha)$ depends on the details of the Hamiltonian and can thus only be established by a consideration of the dynamics involved, which we leave to subsequent work [26], the general behavior will still be similar to the one depicted in Fig. 5.

Neither approximate recoil corrections [34] nor momentum projection and boost [35] are incorporated into the present six-quark calculations. For consistency, the potentials we calculate are therefore normalized with respect to the energy

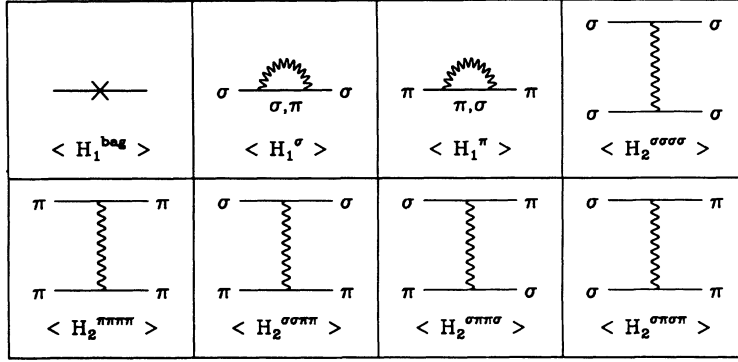


FIG. 4. The various one-body and two-body contributions to the effective Hamiltonian.

$$E_N = \sqrt{M_N^2 + \langle P^2 \rangle}, \quad (30)$$

and not the mass, $M_N = 939$ MeV, of two noninteracting nucleons. The recoil corrections $\langle P^2 \rangle$ stem from the quark wave functions and from the scalar σ field. The two sets of parameters for which the N - N interaction was calculated are given in Table II. For those, the quantity E_N varies between 1145 MeV and 1212 MeV for the sets with $f = \infty$ and $f = 3$, respectively.

Throughout this investigation, the strong coupling constant α_s we use for evaluating the gluonic share of the effective Hamiltonian is obtained by fitting the experimental N - Δ splitting by employing either a free or a “confined” gluonic propagator. The corresponding values for α_s^{free} and α_s^{conf} for the two sets of parameters under consideration are listed in the sixth and seventh columns of Table II, respectively. Thus, when evaluating the color-magnetic hyperfine interaction where, as pointed out in the last section, a free gluonic propagator is used, α_s^{free} is substituted for the strong coupling constant. Correspondingly, α_s^{conf} is used for the color electrostatic part of the interaction where, on the other hand, “confined” gluonic propagators are employed.

In addition, in all actual numerical calculations an in-

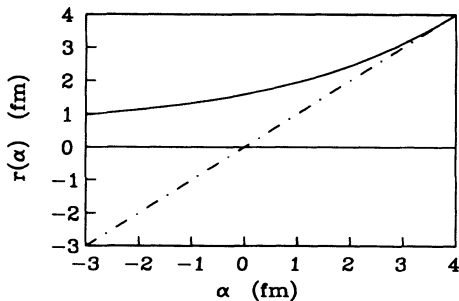


FIG. 5. The internucleon separation r as a function of the deformation parameter α . The figure is taken from Ref. [6] where the Friedberg-Lee soliton model was applied to N - N scattering. Note that no gluonic effects were taken into account in Ref. [6].

frared regularization of the dielectric function $\kappa(\sigma)$ was introduced [16] in order to handle the infinities in the one gluon exchange diagrams associated with a vanishing dielectric constant. We replace $\kappa(\sigma)$ with

$$\kappa(\sigma) \rightarrow \kappa(\sigma)(1 - \kappa_v) + \kappa_v \quad (31)$$

and use $\kappa_v = 0.1$ throughout this investigation. We have convinced ourselves that our final results are stable with respect to variations in this regularization parameter. Note that “intermediate quantities” (e.g., the energies associated with individual diagrams or the strong coupling constant α_s) will, however, well depend on κ_v .

In Figs. 6 and 7 we show the adiabatic N - N potential obtained from a diagonalization of the effective Hamiltonian in the Hilbert space spanned by the six-quark configurations listed in Eq. (20). Results are depicted for the isospin-spin channels $(TS) = (01)$ (Fig. 6) and $(TS) = (10)$ (Fig. 7). For $(TS) = (01)$, the potential can furthermore be split into a central and a tensor part, where [39]

$$V_{\text{cent}}^{(TS)=(01)} = \frac{1}{3} \left(2V_{M=\pm 1}^{(TS)=(01)} + V_{M=0}^{(TS)=(01)} \right), \quad (32a)$$

$$V_{\text{tens}}^{(TS)=(01)} = \frac{1}{6} \left(V_{M=\pm 1}^{(TS)=(01)} - V_{M=0}^{(TS)=(01)} \right). \quad (32b)$$

The central interaction we find is purely repulsive with a “soft” core between 200 MeV ($f = 3$, solid line) and 350 MeV ($f = \infty$, dot-dash line) for the two sets of pa-

TABLE II. Parameter sets for which the adiabatic N - N potential was calculated. The sets are adjusted to yield the proton rms charge radius, the nucleon mass, and the N - Δ mass splitting, where the latter quantity was evaluated employing a free as well as a “confined” gluonic propagator. For further details see Sec. II.

f	a (fm $^{-2}$)	b (fm $^{-1}$)	c	g_0	α_s	α_s^{conf}
					α_s^{free}	α_s^{conf}
3.0	97.45	-1709.9	10000	0.81	3.36	1.42
∞	0.00	-726.1	10000	1.80	3.64	1.50

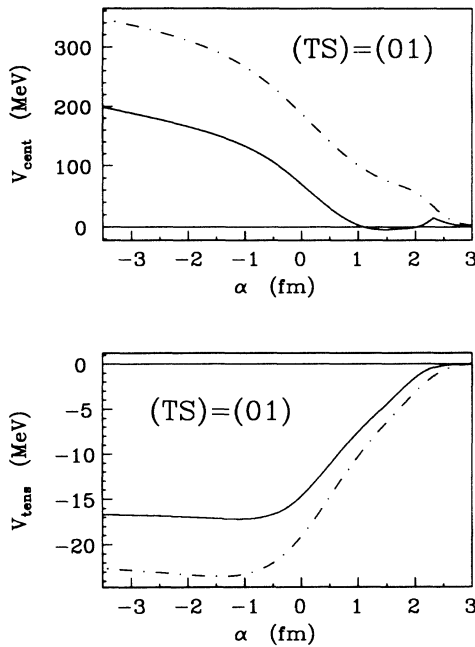


FIG. 6. The adiabatic N - N potential for the isospin-spin channel $(TS) = (01)$ is split into a central [Eq. (32a)] and a tensor part [Eq. (32b)]. The solid line corresponds to the parameter set with $f = 3$ and the dot-dash line to the set with $f = \infty$. Both sets were adjusted to the standard properties of the nucleon and are listed in Table II.

rameters under consideration. As outlined in Sec. II, for $f = 3$ the bag pressure vanishes which leads to hard bags with a thin surface, and $f = \infty$ yields soft bags with a thick surface. This leads to a very different behavior of the surface energy associated with the scalar field, which extends to the variations observed in the interaction. Also, the cusp in the central potential around $\alpha \approx 2.3$ fm for $f = 3$ originates in that surface energy. At that deformation, the scalar field turns abruptly from forming two separated bags to spanning just one united cavity.

An intermediate-range attraction, as observed in earlier calculations of that type (see, e.g., Ref. [5]), is not at all visible in our results. De Tar [5] attributes that to

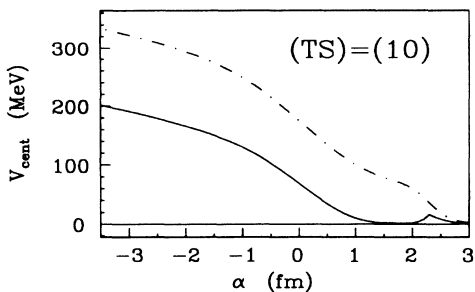


FIG. 7. The adiabatic N - N potential for the isospin-spin channel $(TS) = (10)$. The labeling is the same as in Fig. 6.

the strong color-electrostatic attraction within the quark triplets. Although the color-electrostatic one-gluon exchange diagrams are entirely attractive, in our investigation, their effects are actually more than canceled by the repulsive self-energy diagrams, $\langle H_1^\sigma \rangle$ and $\langle H_1^\pi \rangle$. Note that the color-magnetic self-energies were left out altogether in this investigation. On the other hand, the long- and medium-range N - N attraction should actually be attributed to the meson exchange, and to get a good description of this in a quark model requires the “sea” quarks to be taken into account explicitly [43], which are not accounted for in our investigation at this stage. To cure that shortcoming, we plan [27] to include an explicit pion exchange between the quarks, which will then lead to an effective pionic dressing of the individual nucleons along the lines proposed, e.g., by Miller *et al.* [44].

To determine the relevance of the so-called [37] “hidden-color” states [$|3\rangle$ through $|7\rangle$ in Eq. (20)], which asymptotically fission into color non-singlets, in Fig. 8 we show their relative admixture to the six-quark ground state of the effective Hamiltonian. We observe that their contributions become significant as soon as the nucleonic bags overlap considerably, and that up to 50% of the ground state wave function can actually be made up of “hidden-color” components for small internucleon separations, i.e., oblate deformations. This proves the importance of channel coupling in that realm, and is consistent with the findings of Ref. [21], as corrected in Ref. [45].

The different contributions to the adiabatic N - N potential are analyzed in Figs. 9 and 10 and in Table III.

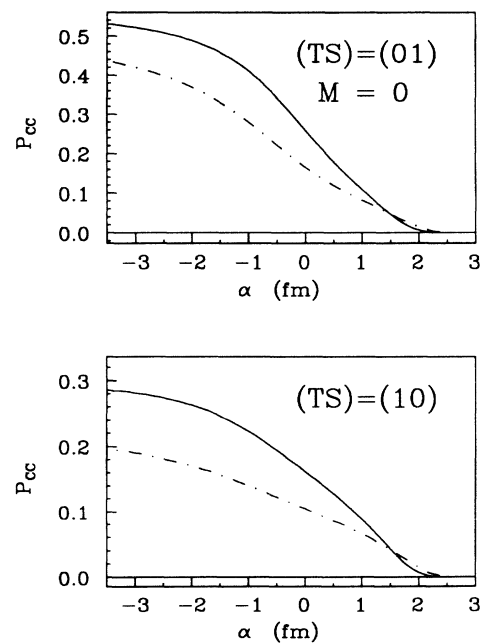


FIG. 8. The admixture of “hidden-color” states, $|3\rangle$ through $|7\rangle$ in Eq. (20), in the ground state of the effective Hamiltonian for two different isospin-spin channels, $(TS) = (01)|_{M=0}$ and $(TS) = (10)$, and for the two sets of parameters listed in Table II. The solid line corresponds to $f = 3$ and the dot-dash line to $f = \infty$.

TABLE III. The contributions to the adiabatic N - N potential stemming from the various diagrams shown in Fig. 4 and given in Eqs. (27) and (29). Results are listed for well separated ($\alpha = 3.5$ fm) as well as completely overlapping nucleonic bags ($\alpha = 0.0$ fm), and also for the adiabatic potential at $\alpha = 0.0$ fm, which is the difference of the latter two quantities. The energies shown correspond to the isospin-spin channel $(TS) = (10)$, and are obtained using the parameter sets given in Table II.

	$f = 3.0$			$f = \infty$		
	$E _{0.0 \text{ fm}}$	$E _{3.5 \text{ fm}}$	$V_{ad}^{NN} _{0.0 \text{ fm}}$	$E _{0.0 \text{ fm}}$	$E _{3.5 \text{ fm}}$	$V_{ad}^{NN} _{0.0 \text{ fm}}$
$\langle H_1^{\text{bag}} \rangle$	93	240	-147	212	256	-44
$\langle H_1^\sigma \rangle$	5849	3757	2092	5506	4685	821
$\langle H_1^\pi \rangle$	2654	3756	-1102	3093	4682	-1589
$\langle H_2^{\sigma\sigma\sigma\sigma} \rangle$	-3728	-1100	-2628	-3222	-1507	-1715
$\langle H_2^{\pi\pi\pi\pi} \rangle$	-901	-1098	197	-1101	-1504	403
$\langle H_2^{\sigma\sigma\pi\pi} \rangle$	-3403	-2504	-899	-3651	-3390	-261
$\langle H_2^{\sigma\pi\pi\sigma} \rangle$	-92	-1402	1310	-144	-1480	1336
$\langle H_2^{\sigma\pi\sigma\pi} \rangle$	-403	-1649	1246	-518	-1742	1224
$\langle H \rangle$	69	0	69	175	0	175

In Fig. 9, we show the various potentials we obtain when employing different approximations for the one gluon exchange. Results are depicted for the isospin-spin channel $(TS) = (01)$ and for a two-nucleon state with the spins aligned antiparallel along the separation axis, i.e., for $M = 0$.

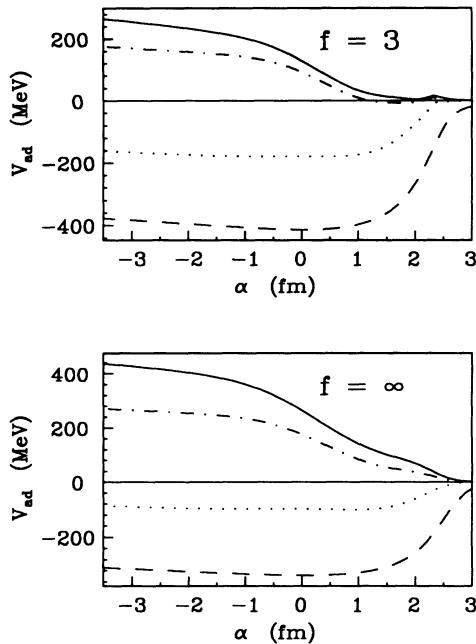


FIG. 9. The various N - N potentials obtained when employing different approximations for the one gluon exchange. Results are shown for the isospin-spin channel $(TS) = (01)|_{M=0}$, and for the two sets of parameters given in Table II. The dashed line corresponds to a calculation where the OGE was omitted altogether, and the dotted line shows the results of a calculation where only the color-magnetic hyperfine interaction was included. The dot-dash and the solid lines correspond to calculations where, in addition, different versions of the color-electrostatic OGE were taken into account. In detail, the solid line shows the results of a calculation employing a “confined” Green’s function, while the dot-dash line corresponds to the use of a free gluonic propagator.

The dashed line in Fig. 9 corresponds to a calculation where the OGE was left out altogether, and in agreement with an earlier investigation [6] where the Friedberg-Lee soliton model without the OGE was applied to N - N scattering, we find a strongly attractive adiabatic potential. The dotted line shows the results of a calculation where the color-magnetic hyperfine interaction was included, which in the literature is quoted as being responsible for the short-range repulsive core [46]. In contrast to that belief, the spin-spin interaction reduces the attraction but does not yield any repulsion. The dot-dash and the solid

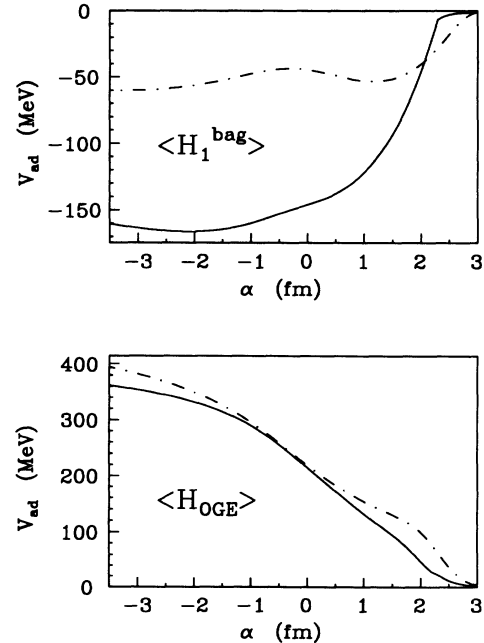


FIG. 10. The adiabatic potential for the isospin-spin channel $(TS) = (10)$ is split into a part independent of the one gluon exchange, $\langle H_1^{\text{bag}} \rangle$ of Eq. (27), and a gluonic contribution $\langle H_{\text{OGE}} \rangle$ of Eq. (29). The solid line corresponds to $f = 3$ and the dot-dash line to $f = \infty$.

line correspond to calculations where, in addition, the color-electrostatic OGE was included, and they indeed yield a repulsive core. In contrast to the solid line, which shows the results of a calculation employing a “confined” scalar Green’s function, the dot-dash line corresponds to the use of a free gluonic propagator, as outlined in Sec. V. The differences between both calculations prove to be rather minute, which gives us confidence that the uncertainties we encounter from evaluating the color-magnetic hyperfine interaction with a free tensor propagator are quite small, as well.

In Fig. 10, the adiabatic potential for the isospin-spin channel $(TS) = (10)$ is split into a gluonic contribution, $\langle H_{\text{OGE}} \rangle$ of Eq. (29), and a part that is independent of the one-gluon exchange $\langle H_1^{\text{bag}} \rangle$ of Eq. (27). The nongluonic contribution (which stems from the single-particle energies, the scalar σ field, and the external potential used to generate the quark wave functions) is always attractive, while the OGE part of the Hamiltonian is purely repulsive. Also, the differences between the two sets of parameters, which we observed in the central adiabatic potentials shown in Figs. 6 and 7, stem almost entirely from $\langle H_1^{\text{bag}} \rangle$, with the “hard” set ($f = 3$, the solid line) being much more attractive. As previously mentioned, the origin of that variation is the very different behavior of the surface energy associated with the scalar σ field for the two sets of parameters under consideration. Despite those differences, their gluonic shares of the energy are very similar.

At this point, a more detailed comparison with De Tar’s [5] pioneering study of the adiabatic two-nucleon interaction in the framework of the MIT bag model is appropriate. As can be seen from Ref. [5], for the MIT bag model, the nongluonic contribution $\langle H_1^{\text{bag}} \rangle$ is repulsive, while the gluonic share of the Hamiltonian, $\langle H_{\text{OGE}} \rangle$, yields all the attraction. This is just opposite to our findings. The difference concerning the nongluonic interaction is due to the very different nature of the surface dynamics of the scalar background field for the MIT and the solitonic bag. The differences in the gluonic share of the Hamiltonian, on the other hand, arise both from the approximations De Tar made in the evaluation of the OGE self-energy terms, and from the differences in the color-dielectric constant (and thus also in the gluonic propagators) between the two models. Also, the six-quark con-

figuration space we are using is much larger than the one De Tar was employing, and his single-quark states are rather artificial constructions, while our “molecular orbitals” are eigenstates of a constrained mean field Hamiltonian.

To get a more detailed understanding of the origins of our results, in Table III we list the various contributions to the adiabatic N - N potential stemming from the individual diagrams shown in Fig. 4. The energies printed are the expectation values of the ground state of the effective Hamiltonian for the isospin-spin channel $(TS) = (10)$. They correspond to the limiting cases of two well-separated nucleons ($\alpha = 3.5$ fm) as well as one united spherically symmetric cavity ($\alpha = 0.0$ fm). The individual OGE mutual interaction terms $\langle H_2^{pqrs} \rangle$ are all attractive, while the self-energy diagrams, $\langle H_1^\sigma \rangle$ and $\langle H_1^\pi \rangle$, are always repulsive. Furthermore, only if the color-electrostatic “off-diagonal” self-energy terms ($\sigma-\pi-\sigma$ and $\pi-\sigma-\pi$) are taken into account is the color-electric flux confined [5] and the interaction vanishes at asymptotic internucleon separations, i.e., $\langle H \rangle \rightarrow 0$ for large α . That this can really be observed in our results (see the third and sixth column in the table) is nontrivial and is a nice confirmation that our numerics are correct. It can also be seen from Table III that the adiabatic potential at vanishing N - N separation arises from significant cancellations between individual terms that are rather large, with the repulsive one gluon exchange contributions overpowering the attractive nongluonic share of the effective Hamiltonian.

For all the results reported in this section, the single-quark wave functions were generated from a scalar potential having a particular shape, as characterized by the geometrical parameters $R(\alpha)$, Γ , and σ_0 [see Eqs. (16)–(18)]. As outlined in Sec. III, the radius of the six-quark bag $R(\alpha)$ is varied as a function of the deformation such that the volume of the σ field cavity remains fixed. In order to test the validity of that approximation, for $\alpha = 0$ we construct self-consistent eigenstates of the total Hamiltonian requiring a spherically symmetric scalar field. In Table IV, we compare results for the geometrical shape parameters and the adiabatic potential, which we find from the self-consistent calculation with the corresponding quantities obtained by using the “constant volume” approach. Results are listed for $(TS) = (01)$

TABLE IV. The geometrical parameters $R(\alpha)$, Γ , and σ_0 , characterizing the field σ_α [see Eqs. (16)–(18)] from which the external scalar potential, \mathcal{V}_α of Eq. (15), is obtained. The quantities shown correspond to the isospin-spin channel $(TS) = (01)|_{M=0}$ and to zero deformation, i.e., $\alpha = 0$ fm. Self-consistent solutions constrained to yield a spherically symmetric scalar field are compared with the “constant volume” approach outlined in Sec. III.

f		R (fm)	Γ (fm $^{-1}$)	σ_0 (fm $^{-1}$)	V_{ad}^{NN} (MeV)
3.0	Constant volume	1.021	4.230	0.4050	128.8
	Self-consistent	1.178	5.548	0.3514	124.2
∞	Constant volume	1.226	2.167	0.2592	264.5
	Self-consistent	1.257	2.032	0.2249	262.3

and $M = 0$. Although the geometrical parameters of the self-consistently determined scalar field are quite different from the ones characterizing σ_α in the “constant volume” approximation, the resulting adiabatic potentials are very similar. This shows that the uncertainties we encounter by choosing this particular path in the configuration space spanned by the geometrical parameters R , Γ , and σ_0 will also be minute and will hence not affect our conclusions.

VII. CONCLUSION AND OUTLOOK

We have evaluated the adiabatic nucleon-nucleon potential in a relativistic quark bag model, which yields spatial as well as color confinement and is free of the spurious color van der Waals forces which trouble most nonrelativistic calculations in that realm. The six-quark system we investigate is confined in a deformed baglike mean field through an effective nonlinear interaction between the quarks and a scalar field. The shape of this confining field is adjusted to reproduce the corresponding quantity for the asymptotic case of two well-separated noninteracting nucleons, and is then varied with deformation treating the scalar field as an incompressible liquid.

Six-quark molecular-type configurations are then generated as a function of deformation, and their energies are evaluated in a coupled channel analysis. By using molecular states instead of cluster model wave functions, we can be sure that all important six-quark configurations are properly considered, a necessary prerequisite for finding reasonable results.

The corresponding effective Hamiltonian includes not only the interaction between the quarks and the scalar background field but also quark-quark interactions generated through one gluon exchange. Furthermore, when calculating the gluonic propagators mediating that interaction, the inhomogeneity and deformation of the dielectric medium were taken into account, and the Coulomb gauge was applied.

Results for the adiabatic local nucleon-nucleon potential have been presented for the different spin-isospin channels which are compatible with $L = 0$ partial waves, and they differ quite considerably from a realistic phenomenological interaction [47] fit to the experimental phase shifts. Although the adiabatic central potentials display a “soft” repulsive core, as is desirable from phenomenology, they totally lack the intermediate-range attraction, which was observed in earlier calculations of

that type and which was attributed to the strong color-electrostatic attraction [5].

Although the color-electrostatic exchange diagrams are also entirely attractive in our investigation, their effects are actually more than canceled by the repulsive gluonic self-energy diagrams. A detailed analysis of the different contributions to the effective Hamiltonian unveils that the nongluonic one-body terms would lead to considerable attraction for vanishing internucleon separation, while the one-gluon exchange (mutual and self-interaction) terms produce all the repulsion. To be more specific, in our case it is the color-electrostatic one gluon exchange which leads to the repulsion at small N - N separations, and not the spin-spin color-magnetic hyperfine interaction, which in the literature [46] is quoted as being responsible for the short-range repulsive core.

Considering that the long- and medium-range nucleon-nucleon attraction should actually be attributed to explicit meson exchange and not to quark rearrangement, we are not at all surprised to be missing a good description of this part of the interaction in a quark model which does not include the “sea” quarks. We plan to overcome that detriment by either including quantum surface fluctuations, which would introduce configurations of the form $q^7\bar{q}$ in addition to our q^6 basis states, or by considering an explicit pion exchange between the individual quarks along the lines followed in the cloudy bag model [44]. The latter mechanism is favorable as it also leads to a restoration of the explicitly broken chiral symmetry. Work in that direction is currently in progress [27].

We also plan [26] to account for the dynamics of the N - N interaction by extending this work through means of the generator coordinate method. It has been shown that a significant part of the short-range N - N repulsion is due to dynamics [6], and that the absence of a repulsive core in some early calculations was an artifact of the adiabatic approximation [23,24]. In addition, the effective N - N interaction is highly nonlocal in terms of the separation parameter.

ACKNOWLEDGMENTS

We wish to thank P. Tang and S. Hartmann for many useful discussions. This work was supported in part by the U.S. Department of Energy, by the Deutsche Forschungsgemeinschaft (W.K.), and by the Feodor-Lynen program of the Alexander von Humboldt-Stiftung (W.K.).

[1] H. Yukawa, Proc. Phys. Math. Soc. Jpn. **17**, 48 (1935).
 [2] R. Machleidt, Adv. Nucl. Phys. **19**, 189 (1989).
 [3] H. Markum, M. Meinhart, G. Eder, M. Faber, and H. Leeb, Phys. Rev. D **31**, 2029 (1985).
 [4] D.A. Libermann, Phys. Rev. D **16**, 1542 (1977).
 [5] C.E. De Tar, Phys. Rev. D **17**, 323 (1977).
 [6] A. Schuh, H.J. Pirner, and L. Willets, Phys. Lett. B **174**, 10 (1986).
 [7] G. Kaelbermann, J.M. Eisenberg, R.R. Silbar, and M.M.

Sternheim, Phys. Lett. B **179**, 4 (1986); G. Kaelbermann and J.M. Eisenberg, *ibid.* **188**, 311 (1987).
 [8] T.S. Walhout and J. Wambach, Phys. Rev. Lett. **67**, 314 (1991).
 [9] N.R. Walet, R.D. Amado, and A. Hosaka, Phys. Rev. Lett. **68**, 3849 (1992).
 [10] M. Oka and K. Yazaki, *Quarks and Nuclei*, International Review of Nuclear Physics Vol. 1, edited by W. Weise (World Scientific, Singapore, 1984), p. 489.

- [11] F. Myhrer and J. Wroldsen, *Rev. Mod. Phys.* **60**, 629 (1988).
- [12] K. Shimizu, *Rep. Prog. Phys.* **52**, 1 (1989).
- [13] M. Born and J.R. Oppenheimer, *Ann. Phys.* **84**, 457 (1927).
- [14] M. Oka and K. Yazaki, *Prog. Theor. Phys.* **66**, 556 (1981); **66**, 572 (1981).
- [15] M. Cvetič, B. Golli, N. Mankoc-Borstnik, and M. Rosina, *Nucl. Phys.* **A395**, 349 (1983).
- [16] G. Fai, R.J. Perry, and L. Wilets, *Phys. Lett. B* **208**, 1 (1988).
- [17] G. Krein, P. Tang, L. Wilets, and A.G. Williams, *Phys. Lett. B* **212**, 362 (1988); *Nucl. Phys.* **A523**, 548 (1991).
- [18] R.S. Willey, *Phys. Rev. D* **18**, 270 (1978); P.M. Fishbane and M.T. Grisaru, *Phys. Lett.* **74B**, 98 (1978); S. Matsuyama and H. Miyazawa, *Prog. Theor. Phys.* **61**, 942 (1979); O.W. Greenberg and H.J. Lipkin, *Nucl. Phys.* **A370**, 349 (1981).
- [19] Fl. Stancu and L. Wilets, *Phys. Rev. C* **36**, 726 (1987).
- [20] Fl. Stancu and L. Wilets, *Phys. Rev. C* **38**, 1145 (1988).
- [21] Fl. Stancu and L. Wilets, *Phys. Rev. C* **40**, 1901 (1989).
- [22] D.L. Hill and J.A. Wheeler, *Phys. Rev.* **89**, 1102 (1953); J.J. Griffin and J.A. Wheeler, *ibid.* **108**, 311 (1957).
- [23] A. Faessler, F. Fernandez, G. Lübeck, and K. Shimizu, *Nucl. Phys.* **A402**, 555 (1983).
- [24] M. Harvey, J. LeTourneux, and B. Lorazo, *Nucl. Phys.* **A424**, 428 (1984).
- [25] M. Oka and K. Yazaki, *Nucl. Phys.* **A402**, 477 (1983).
- [26] S. Pepin, W. Koepf, L. Wilets, and Fl. Stancu (unpublished).
- [27] W. Koepf and L. Wilets (unpublished).
- [28] R. Friedberg and T.D. Lee, *Phys. Rev. D* **15**, 1694 (1977).
- [29] A. Chodos, R.L. Jaffe, K. Johnson, C.B. Thorn, and V.F. Weisskopf, *Phys. Rev. D* **9**, 3471 (1974).
- [30] H.B. Nielsen and A. Patkos, *Nucl. Phys.* **B195**, 137 (1982); G. Chanfray, O. Nachtmann, and H.J. Pirner, *Phys. Lett.* **147B**, 249 (1984).
- [31] L. Wilets, *Nontopological Solitons* (World Scientific, Singapore, 1989).
- [32] L. Wilets, S. Hartmann, and P. Tang, "The Chiral Chromodielectric Model: Quark Self Energy and Hadron Bags," University of Washington report, 1993 (unpublished).
- [33] R. Goldflam and L. Wilets, *Phys. Rev. D* **25**, 1951 (1982).
- [34] J.-L. Dethier, R. Goldflam, E.M. Henley, and L. Wilets, *Phys. Rev. D* **27**, 2191 (1983); M. Betz and R. Goldflam, *ibid.* **28**, 2848 (1983).
- [35] E.G. Lübeck, E.M. Henley, and L. Wilets, *Phys. Rev. D* **35**, 2809 (1987).
- [36] M. Bickeboeller, M.C. Birse, H. Marschall, and L. Wilets, *Phys. Rev. D* **31**, 2892 (1985).
- [37] M. Harvey, *Nucl. Phys.* **A352**, 301 (1981); **A352**, 326 (1981).
- [38] K.T. Hecht and S.C. Pang, *J. Math. Phys.* **10**, 1571 (1969); S.I. So and S.D. Strottman, *ibid.* **20**, 153 (1979).
- [39] P. Ring and P. Schuck, *The Nuclear Many-Body Problem* (Springer, New York, 1980).
- [40] M. Bickeboeller, R. Goldflam, and L. Wilets, *J. Math. Phys.* **26**, 1810 (1985).
- [41] P. Tang and L. Wilets, *J. Math. Phys.* **31**, 1661 (1991).
- [42] J. Wroldsen and F. Myhrer, *Z. Phys. C* **25**, 59 (1984).
- [43] J.F. Donoghue and E. Golowich, *Phys. Rev. D* **15**, 3421 (1977).
- [44] S. Théberge, A.W. Thomas, and G.A. Miller, *Phys. Rev. D* **22**, 2838 (1980); A.W. Thomas, S. Théberge, and G.A. Miller, *ibid.* **24**, 216 (1981); S. Théberge and A.W. Thomas, *Nucl. Phys.* **A393**, 252 (1983).
- [45] Fl. Stancu and L. Wilets, "Symmetries of Six-Quark States Related to the Nucleon-Nucleon Problem," Proceedings of the Many Body Conference, Coimbra, Portugal, 1993, edited by C. Fiolhais, M. Fiolhais, C. Sousa, and J.N. Urbano (World Scientific, Singapore, 1994).
- [46] T. Barnes, S. Capstick, M.D. Kovarik, and E.S. Swanson, *Phys. Rev. C* **48**, 539 (1993).
- [47] R.V. Reid, Jr., *Ann. Phys. (N.Y.)* **50**, 411 (1968).